© 2015. Published by The Company of Biologists Ltd | Journal of Cell Science (2015) 128, 2330-2338 doi:10.1242/jcs.167270

RESEARCH ARTICLE

CALHM1 ion channel elicits amyloid-β clearance by insulin-degrading enzyme in cell lines and *in vivo* in the mouse brain

Valérie Vingtdeux[1,2,*,‡,§], Pallavi Chandakkar[1,2], Haitian Zhao[1,2], Lionel Blanc[2], Santiago Ruiz[1,2] and Philippe Marambaud[1,2,¶]

ABSTRACT

Alzheimer's disease is characterized by amyloid-β (Aβ) peptide accumulation in the brain. CALHM1, a cell-surface Ca^{2+} channel expressed in brain neurons, has anti-amyloidogenic properties in cell cultures. Here, we show that CALHM1 controls Aβ levels *in vivo* in the mouse brain through a previously unrecognized mechanism of regulation of Aβ clearance. Using pharmacological and genetic approaches in cell lines, we found that CALHM1 ion permeability and extracellular Ca^{2+} were required for the Aβ-lowering effect of CALHM1. Aβ level reduction by CALHM1 could be explained by an increase in extracellular Aβ degradation by insulin-degrading enzyme (IDE), extracellular secretion of which was strongly potentiated by CALHM1 activation. Importantly, *Calhm1* knockout in mice reduced IDE enzymatic activity in the brain, and increased endogenous Aβ concentrations by up to ∼50% in both the whole brain and primary neurons. Thus, CALHM1 controls Aβ levels in cell lines and *in vivo* by facilitating neuronal and Ca^{2+}-dependent degradation of extracellular Aβ by IDE. This work identifies CALHM1 ion channel as a potential target for promoting amyloid clearance in Alzheimer's disease.

KEY WORDS: CALHM1, Ion channel, Amyloid-β peptide, Insulin-degrading enzyme, Secretion, Alzheimer's disease

INTRODUCTION

Alzheimer's disease is a neurodegenerative brain disorder and the first cause of dementia in elderly individuals. The cerebral extraneuronal lesions called senile plaques represent a defining histopathological characteristic of Alzheimer's disease (Duyckaerts et al., 2009; Serrano-Pozo et al., 2011). Senile plaques are formed by the deposition of amyloid-β (Aβ), a series of peptides produced by sequential endoproteolysis of the amyloid precursor protein (APP) by the action of two proteases, β- and γ-secretases (De Strooper et al., 2010; Haass and Selkoe, 2007; Marambaud and Robakis, 2005). This histological feature, together with concordant genetic and biochemical evidence, support the hypothesis that Aβ is a causative factor in Alzheimer's disease pathogenesis (Hardy and Selkoe, 2002). Notably, most of the familial forms of Alzheimer's disease have been found to be caused by mutations in the genes coding for APP or presenilins (the γ-secretase catalytic components), and some of these pathogenic mutations directly increase Aβ production, favor an increase in the relative abundance of the more neurotoxic Aβ isoform Aβ42 or change Aβ aggregation propensity (Lambert and Amouyel, 2011). Furthermore, recent work has demonstrated the existence of a protective mutation in APP in a large Icelandic Alzheimer's disease cohort (Jonsson et al., 2012) that lowers both production and aggregation of Aβ (Benilova et al., 2014; Maloney et al., 2014). In this context, there is strong interest in identifying selective interventions aimed at preventing or lowering Aβ accumulation in the Alzheimer's disease brain (Citron, 2010).

The calcium homeostasis modulator protein 1 (*CALHM1*) gene (Dreses-Werringloer et al., 2008) was identified by using an expression profiling method (Aguilar et al., 2008), which screened for genes that: (1) were preferentially expressed in the hippocampus – a brain region affected at the early stages of Alzheimer's disease (de Leon et al., 2007) – and (2) were located on susceptibility loci for Alzheimer's disease. *CALHM1* does not appear to be a risk gene for Alzheimer's disease, but independent genetic studies have shown that it influences the onset of Alzheimer's disease (Dreses-Werringloer et al., 2008; Lambert et al., 2010). CALHM1 has also been proposed to control Aβ levels in cell cultures (Dreses-Werringloer et al., 2008; Vingtdeux et al., 2014) and in human cerebrospinal fluid (CSF) (Kauwe et al., 2010; Koppel et al., 2011, but see also Giedraitis et al., 2010). Taken together, these data warrant further investigation aimed at determining whether CALHM1 is involved in molecular mechanisms relevant to Alzheimer's disease pathogenesis (Berridge, 2010).

CALHM1 is expressed in the human and mouse brains, and in hippocampal and cortical neurons (Dreses-Werringloer et al., 2008, 2013; Ma et al., 2012). CALHM1 function in brain neurons remains incompletely understood. Several studies have determined, however, that CALHM1 is a voltage-gated pore-forming protein that forms a plasma membrane Ca^{2+}-permeable channel regulated by extracellular Ca^{2+} concentration (Dreses-Werringloer et al., 2008; Ma et al., 2012; Tanis et al., 2013). Its expression and activation in different cell systems induce Ca^{2+} influx and elevate cytoplasmic Ca^{2+} concentration in response to a drop in extracellular Ca^{2+} concentration (Dreses-Werringloer et al., 2008, 2013). In mouse cortical neurons, CALHM1 responds to extracellular Ca^{2+} not only by elevating intraneuronal Ca^{2+} levels, but also by controlling cell excitability (Ma et al., 2012). Work performed in CALHM1-transfected hippocampal HT-22 cells, as well as wild type (WT) and *Calhm1*-knockout (KO) primary neurons, have further demonstrated that CALHM1-mediated Ca^{2+} influx controls intracellular Ca^{2+} signal transduction (Dreses-Werringloer et al., 2013). Thus, CALHM1 plays a key role in cerebral neuronal Ca^{2+} homeostasis and regulates neuronal function.

In the present study, we show that CALHM1 controls Aβ metabolism, in cell cultures and *in vivo* in the mouse brain, by facilitating a neuronal and Ca^{2+}-dependent mechanism of extracellular clearance of Aβ. Aβ steady-state levels in the brain are known to be the result of a balance between its production from APP and its degradation by efficient clearance mechanisms. Aβ clearance is

[1]Litwin-Zucker Research Center for the Study of Alzheimer's Disease, Manhasset, New York 11030 USA. [2]The Feinstein Institute for Medical Research, Manhasset, New York 11030 USA.
*Present address: Inserm, UMR-S1172 Jean-Pierre Aubert Research Centre, Lille, France. ‡Present address: Université de Lille, Faculté de Médecine, Lille, France. §Present address: CHRU, Lille, France.

¶Author for correspondence (PMaramba@nshs.edu)

Received 9 December 2014; Accepted 18 May 2015

Journal of Cell Science

Journal of Cell Science (2015) 128, 2330-2338 doi:10.1242/jcs.167270

controlled by various pathways, which include endocytosis by several brain cell types (including glia and neurons), protein transport and/or binding mechanisms across the blood–brain barrier, and extracellular enzymatic degradation (Pflanzner et al., 2010; Zolezzi et al., 2014). In the enzymatic pathway, Aβ can be degraded *in vivo* by at least four peptidases from the metallopeptidase family: neprilysin (NEP, also known as MME), endothelin-converting enzyme-1 and -2 (ECE-1 and ECE-2) and insulin-degrading enzyme (IDE) (Turner and Nalivaeva, 2007). Here, we also report that CALHM1 activation lowered extracellular Aβ levels by promoting Aβ clearance by IDE through a mechanism facilitating IDE secretion. This work reveals a previously unrecognized function of CALHM1 in neurons, and identifies the CALHM1 ion channel as an endogenous regulator of Aβ degradation in the brain.

RESULTS

CALHM1 ion channel and extracellular Ca^{2+} control Aβ levels

CALHM1 permeability is regulated by the extracellular Ca^{2+} concentration ($[Ca^{2+}]_o$) (Dreses-Werringloer et al., 2008; Ma et al., 2012). We initially reported that CALHM1 can be activated in cell cultures by a procedure that consists of transiently removing extracellular Ca^{2+} and subsequently adding it back at physiological concentration to create a driving force for Ca^{2+} entry into the cells (Dreses-Werringloer et al., 2008). This procedure, termed the 'Ca^{2+} add-back' condition, induces CALHM1-mediated Ca^{2+} influx and elevates intracellular Ca^{2+} concentration ($[Ca^{2+}]_i$). An analysis of the relationship between the CALHM1-mediated increase of $[Ca^{2+}]_i$ and CALHM1 channel activity revealed that CALHM1 is strongly regulated by $[Ca^{2+}]_o$ and is activated by a drop in $[Ca^{2+}]_o$, with a half-maximal activation concentration of ~0.2 mM Ca^{2+} (Ma et al., 2012). Concordant studies have demonstrated that normal electrical activity in neurons can result in a robust drop of $[Ca^{2+}]_o$ (up to concentrations <0.1 mM) in the interstitium and synaptic clefts of the brain (Rusakov and Fine, 2003). Thus, neuronal activity reduces $[Ca^{2+}]_o$ within the range of CALHM1 activation (Ma et al., 2012). In this context, and in order to use a more physiologically relevant procedure of CALHM1 activation than the Ca^{2+} add-back condition, we tested the effect of directly incubating the cells in artificial cerebrospinal fluid (aCSF) buffer containing 0.2 mM Ca^{2+}.

Using Fluo-4 $[Ca^{2+}]_i$ measurements, we found that lowering $[Ca^{2+}]_o$ from 1.4 mM (physiological concentration) to 0.2 mM (half-maximal CALHM1 activation concentration) led to a significant increase in $[Ca^{2+}]_i$ in CALHM1-transfected cells, compared to control cells (Fig. 1A,B), confirming that Ca^{2+} influx through CALHM1 was observed in these conditions. The effect of CALHM1 activation on $[Ca^{2+}]_i$ was observed ∼5 min after switching to 0.2 mM Ca^{2+} buffer, but only once $[Ca^{2+}]_i$ stabilized after the drop generated by the decrease in $[Ca^{2+}]_o$ (Fig. 1A). Importantly, application of 0.2 mM Ca^{2+} aCSF also resulted in a strong reduction of extracellular Aβ accumulation in cells transfected with either human or mouse CALHM1, compared to vector-transfected control cells (Fig. 1C). These results are in line with our previous findings showing that the Ca^{2+} add-back condition lowers Aβ accumulation in CALHM1-expressing cells (Dreses-Werringloer et al., 2008; Vingtdeux et al., 2014), and further demonstrate that the effect of CALHM1 on $[Ca^{2+}]_i$ parallels its inhibitory effect on Aβ accumulation.

We next asked whether the ion channel properties of CALHM1 are required for its inhibitory effect on Aβ levels. CALHM1 permeability can be modulated pharmacologically or genetically. No specific CALHM1 ion channel blocker has been identified yet. However, the non-specific inorganic dye Ruthenium Red or the ion Zn^{2+} can fully inhibit CALHM1 currents and CALHM1-mediated $[Ca^{2+}]_i$ increase (Dreses-Werringloer et al., 2013; Ma et al., 2012). Ruthenium Red and Zn^{2+}, at concentrations inhibiting CALHM1 permeability (Dreses-Werringloer et al., 2013; Ma et al., 2012), blocked the effect of CALHM1 on Aβ accumulation (Fig. 1D,E).

CALHM1 is N-glycosylated at residue Asp140 to yield a second immunoreactive band on western blots, and mutation of Asp140 to an alanine residue (N140A) prevents both CALHM1 N-glycosylation and CALHM1-mediated Ca^{2+} influx (Dreses-Werringloer et al., 2008, 2013). Two conserved residues in the third hydrophobic domain of CALHM1, Trp114 (Dreses-Werringloer et al., 2013) and Asp121 (Ma et al., 2012), have also been identified as being potentially important for pore formation and/or ion permeation of the channel. Indeed, mutation of Trp114 to an alanine residue (W114A) and Asp121 to an arginine residue (D121R) have been found to fully block CALHM1-mediated Ca^{2+} influx (Dreses-Werringloer et al., 2013) and CALHM1 currents (Ma et al., 2012), respectively. Fig. 1F shows that, compared to WT CALHM1, the three functionally defective CALHM1 mutants, N140A, W114A and D121R, all failed to reduce Aβ levels. The lack of effect of these three mutants on Aβ accumulation could not be explained by defects in CALHM1 protein expression or stability (Fig. 1F).

We then determined whether extracellular Ca^{2+} is required for the effect of CALHM1 on Aβ levels. As expected, CALHM1-mediated Ca^{2+} influx in 0.2 mM Ca^{2+} aCSF could be inhibited by the chelating agent EGTA (2 mM, see Fig. 1G). In these conditions, the effect of CALHM1 activation on Aβ levels was also noticeably blocked (Fig. 1I). Addition of a saturating concentration of Ca^{2+} (5 mM) in EGTA-containing 0.2 mM Ca^{2+} aCSF restored the effect of CALHM1 on both $[Ca^{2+}]_i$ (Fig. 1G,H) and Aβ levels (Fig. 1I). Taken together, these results show that functional CALHM1 ion channels and Ca^{2+} influx through CALHM1 control Aβ levels.

CALHM1 promotes extracellular Aβ degradation by a soluble proteolytic activity

The effect of CALHM1 on Aβ levels could be due to a decrease in Aβ production from APP or to an increase in intracellular or extracellular Aβ degradation (Leissring and Turner, 2013). We observed no reduction in intracellular Aβ levels upon conditions of CALHM1 expression and activation in 0.2 mM Ca^{2+} aCSF (Fig. 2A). Moreover, treatment with the lysosomotropic drugs NH_4Cl and chloroquine, which neutralize Aβ lysosomal degradation (Nixon et al., 2008; Vingtdeux et al., 2010), did not prevent the decrease of extracellular Aβ by CALHM1 (Fig. 2A).

We next assessed the effect of CALHM1 on the rate of Aβ production. To this end, we used the approach of transient block of protein transport through the secretory pathway by the reversible Golgi disassembling agent brefeldin A (BFA) (Langhans et al., 2007). As well as having well-established reversible effects on cellular trafficking, BFA has the advantage of specifically interrupting the export of newly synthesized proteins from the ER (Lippincott-Schwartz et al., 1989) without affecting protein synthesis, including APP synthesis (Knops et al., 1993). As we previously observed, BFA induced the accumulation of APP in the ER (Chapuis et al., 2011) and completely inhibited intracellular and extracellular Aβ accumulation (Fig. 2B,C). BFA washout allowed the reactivation of APP trafficking to progressively restore APP processing and Aβ production (Fig. 2B). We found no effect of CALHM1 expression and its activation on the rate of restoration of Aβ production, whereas, as expected, extracellular Aβ accumulation was strongly inhibited by CALHM1 activation (Fig. 2C). Thus,

Journal of Cell Science

Journal of Cell Science (2015) 128, 2330-2338 doi:10.1242/jcs.167270

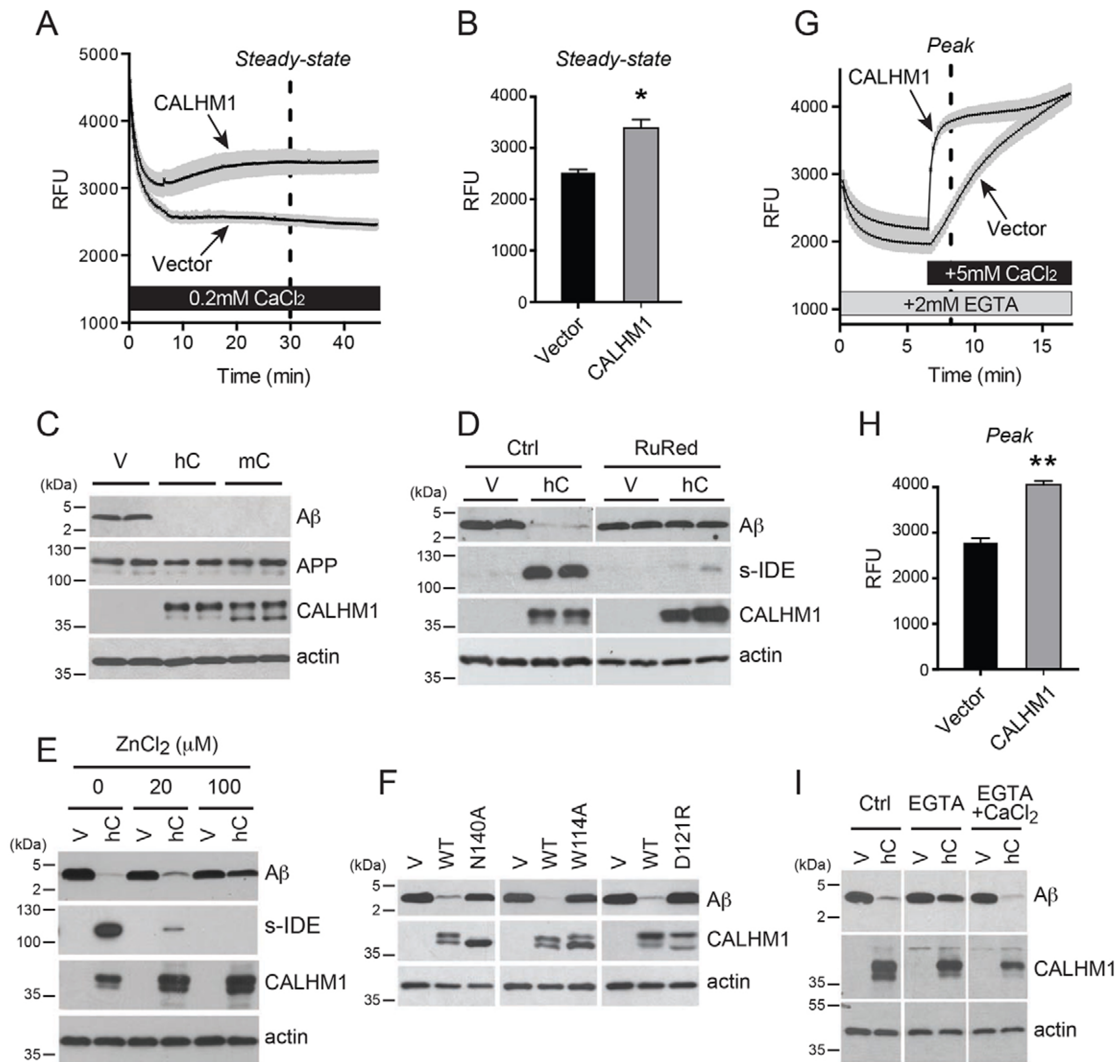

Fig. 1. CALHM1 ion channel activation and extracellular Ca^{2+} control secreted Aβ levels. (A) $[Ca^{2+}]_i$ measurements with Fluo-4 in HT-22 cells transfected with human CALHM1 or control empty vector. Cells were incubated in aCSF containing CALHM1-activating $[Ca^{2+}]_o$ (0.2 mM $CaCl_2$). Traces illustrate the mean relative fluorescence units (RFUs) ±s.e.m. (shaded areas) of three independent experiments. (B) Steady-state of $[Ca^{2+}]_i$ measurements as in A, expressed in RFUs (mean±s.e.m.; **P*<0.05; *n*=3; unpaired Student's *t*-test with Welch's correction). (C) APP-N2a cells transfected with control vector (V), human CALHM1 (hC) or mouse CALHM1 (mC) were incubated in 0.2 mM $CaCl_2$ aCSF for 1 h to activate CALHM1. Secreted total Aβ and cellular APP, CALHM1 and actin were analyzed by western blotting. (D,E) APP-N2a cells transfected with control vector (V) or CALHM1 (hC) were preincubated or not for 30 min with Ruthenium Red (RuRed, 20 µM, D) or the indicated concentrations of $ZnCl_2$ (E). Cells were then stimulated with 0.2 mM $CaCl_2$ aCSF for 1 h in the presence or absence of RuRed or $ZnCl_2$ and analyzed by western blotting for the indicated proteins. Secreted extracellular IDE (s-IDE) was also analyzed by western blotting. (F) APP-N2a cells were transfected with control vector (V), or WT-, N140A-, W114A- or D121R-CALHM1. Cells were then stimulated with 0.2 mM $CaCl_2$ aCSF and analyzed as in C. (G) $[Ca^{2+}]_i$ measurements with Fluo-4 in HT-22 cells transfected with CALHM1 or control vector as in A. $[Ca^{2+}]_i$ was monitored in cells first incubated in 0.2 mM $CaCl_2$ aCSF supplemented with 2 mM EGTA and then challenged with 5 mM $CaCl_2$, as indicated in the graph. Traces illustrate the mean±s.e.m. (shaded areas) RFUs of three independent experiments. (H) Peak of $[Ca^{2+}]_i$ measurements as in G, expressed in RFUs (mean±s.e.m.; ***P*<0.001; *n*=3; unpaired Student's *t*-test with Welch's correction). (I) APP-N2a cells transfected with control vector (V) or CALHM1 (hC) were stimulated with 0.2 mM $CaCl_2$ aCSF for 30 min in the absence or presence of 2 mM EGTA. Cells were then challenged or not with 5 mM $CaCl_2$ (+$CaCl_2$) for 30 min and analyzed by western blotting as in C. Western blotting results in C–F and I are representative of at least three independent experiments.

CALHM1 had no effect on either Aβ production or intracellular Aβ degradation by the lysosomes.

We then investigated whether CALHM1 promotes extracellular Aβ degradation and whether a membrane-associated or soluble proteolytic activity is involved in this mechanism. In a cell-free assay, we incubated (37°C) the conditioned medium of CALHM1-transfected cells (which were activated in 0.2 mM Ca^{2+} aCSF) with exogenous Aβ from the conditioned medium of APP-transfected cells (see Fig. 2D). In these conditions, we observed a substantial degradation of exogenous Aβ by the conditioned medium of cells expressing activated CALHM1, whereas the conditioned medium of non-transfected cells or cells transfected with a control vector had no effect on Aβ levels (Fig. 2E). These data show that upon CALHM1 activation, Aβ is targeted for degradation in the extracellular space by a soluble proteolytic activity.

CALHM1 promotes extracellular Aβ degradation through IDE

Extracellular Aβ proteolytic clearance is mediated *in vivo* by at least four peptidases from the metallopeptidase family: NEP, ECE-1, ECE-2 and IDE (Turner and Nalivaeva, 2007). Treatment with

Journal of Cell Science

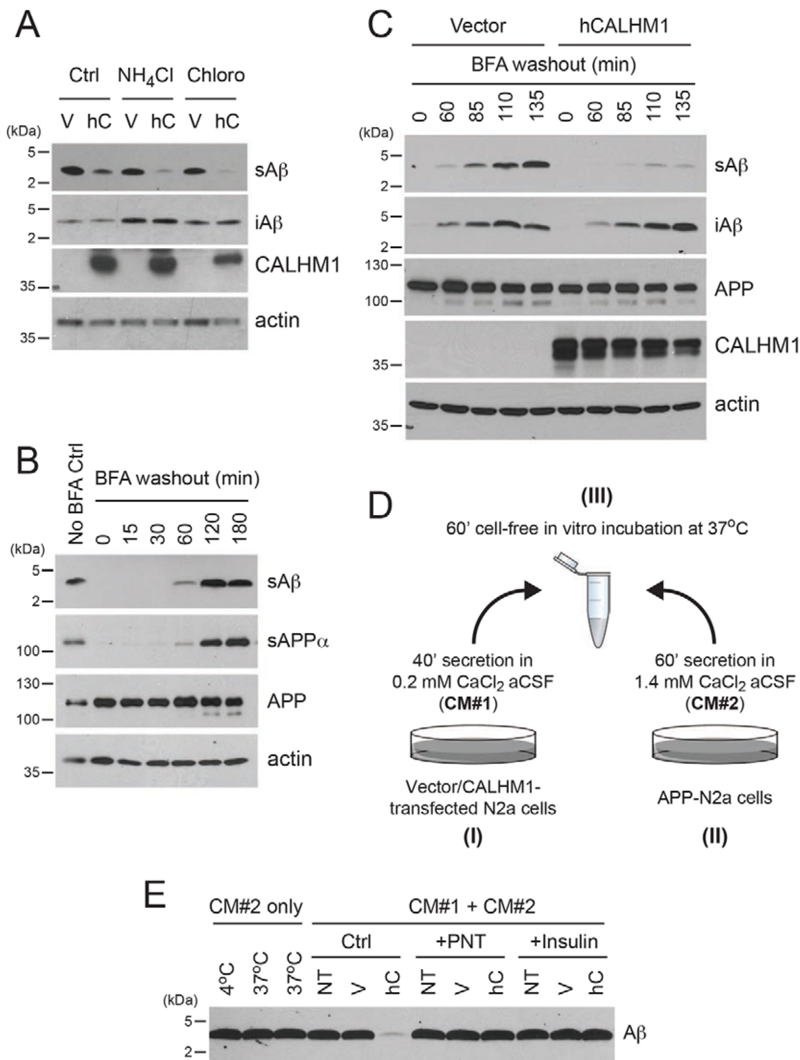

Fig. 2. CALHM1 promotes extracellular Aβ degradation by a soluble proteolytic activity. (A) APP-N2a cells transfected with control vector (V) or human CALHM1 (hC) were preincubated or not for 30 min with NH_4Cl (10 mM) or chloroquine (Chloro, 50 µM). Cells were then stimulated for 1 h with 0.2 mM $CaCl_2$ aCSF supplemented or not with the different inhibitors. Secreted Aβ (sAβ) and cellular CALHM1 and actin were analyzed by western blotting. Intracellular Aβ (iAβ) was analyzed by immunoprecipitation and western blotting. (B) APP-N2a cells were treated or not (No BFA Ctrl) with brefeldin A (BFA, 1 µg/ml) for 3 h. BFA was then removed by washing and incubating the cells in complete culture medium for the indicated times to allow recovery of APP trafficking and maturation (BFA washout). Secreted Aβ (sAβ) and APPα (sAPPα) and cellular APP and actin were analyzed by western blotting. (C) APP-N2a cells transfected with control vector or human CALHM1 (hCALHM1) were treated with BFA as in B. Cells were then washed and stimulated with 0.2 mM $CaCl_2$ aCSF for the indicated times (BFA washout). Secreted Aβ (sAβ) and cellular APP, CALHM1, and actin were analyzed by western blotting. Intracellular Aβ (iAβ) was analyzed by immunoprecipitation and western blotting. (D) Schematic description of the cell-free assay used in E. Naïve N2a cells transfected with control vector or CALHM1 were stimulated with 0.2 mM $CaCl_2$ aCSF for 40 min (I). Conditioned medium (CM#1) was harvested and combined with APP-N2a cell conditioned medium (CM#2, II). Combined conditioned media were incubated for 60 min at 37°C to assess Aβ degradation (III). (E) Cell-free assay performed as in D by combining the conditioned medium (CM#1) from naïve N2a cells that were either non-transfected (NT), or transfected with control vector (V) or human CALHM1 (hC), with APP-N2a cell conditioned medium (CM#2). The assay was performed in the absence (Ctrl) or presence of 1,10-phenanthroline (PNT, 2 mM) or insulin (25 µM). As controls, APP-N2a cell conditioned medium was incubated separately *in vitro* (CM#2 only) at 4°C or 37°C to assess Aβ stability during the assay in the absence of CM#1. After incubation, Aβ levels were analyzed by western blotting. Western blotting results in A–C and E are representative of three independent experiments.

phosphoramidon, which inhibits NEP and ECEs, or with thiorphan, which is more specific for NEP inhibition, failed to prevent the effect of CALHM1 on Aβ (Fig. 3A,D). In contrast, 1,10-phenanthroline (PNT), which inhibits IDE, or insulin, which acts as a potent competitive inhibitor for Aβ degradation by IDE, fully blocked Aβ degradation by CALHM1-transfected cells (Fig. 3B–D). The inhibitory effect of PNT and insulin on CALHM1-mediated Aβ degradation was also observed *in vitro* in the cell-free assay using the conditioned medium of CALHM1-transfected cells (Fig. 2E). Because Aβ can be degraded by PNT- and insulin-sensitive proteolytic activities independently of IDE (Espuny-Camacho et al., 2010), we verified the implication of IDE in this mechanism by directly targeting IDE expression using small interfering RNAs (siRNAs). We found that IDE expression reduction by RNA interference (RNAi) lowered the effect of CALHM1 on Aβ degradation (Fig. 3E), confirming that IDE mediates Aβ degradation upon CALHM1 activation.

Because our data incriminate extracellular soluble IDE in CALHM1-mediated Aβ degradation, we analyzed IDE levels in the conditioned medium of CALHM1-transfected cells. We found that CALHM1 transfection and its activation in 0.2 mM Ca^{2+} aCSF triggered a substantial secretion of IDE from different cell lines, such as N2a (expressing or not human APP) and HT-22 cells (Fig. 3F, see also Fig. 3E). Importantly, IDE secretion was fully blocked by conditions that inhibit CALHM1 permeability, such as Ruthenium Red and Zn^{2+} treatments (Fig. 1D,E) or expression of the functionally defective CALHM1 mutant W114A-CALHM1 (Fig. 3G). Taken together, these results show that CALHM1 ion channel promotes extracellular Aβ degradation by IDE through an increase in IDE secretion.

CALHM1 deficiency decreases IDE activity in the mouse brain

To determine whether CALHM1 controls cerebral IDE activity, we first assessed the *in vitro* degradation of exogenous Aβ and insulin by *Calhm1* KO and WT brain homogenates. *Calhm1*-KO mice were recently generated in our laboratory and are viable and fertile (Dreses-Werringloer et al., 2013; Ma et al., 2012; Taruno et al., 2013). Histological analyses have revealed that *Calhm1* KO mice display no defects in brain development or brain integrity in adulthood (P.M. and V.V. unpublished observations), which make them a relevant model to study CALHM1 functions in the brain.

IDE is secreted but can also be found as a membrane-bound enzyme outside the cell (Vekrellis et al., 2000). Soluble and membrane-associated brain homogenates were prepared from adult WT (*Calhm1*$^{+/+}$) and *Calhm1*-KO (*Calhm1*$^{-/-}$) mice, and were analyzed for synthetic Aβ and recombinant insulin degradation in an *in vitro* assay (see Materials and Methods). Strikingly, both soluble and membrane-associated brain homogenates contained significantly

Journal of Cell Science (2015) 128, 2330-2338 doi:10.1242/jcs.167270

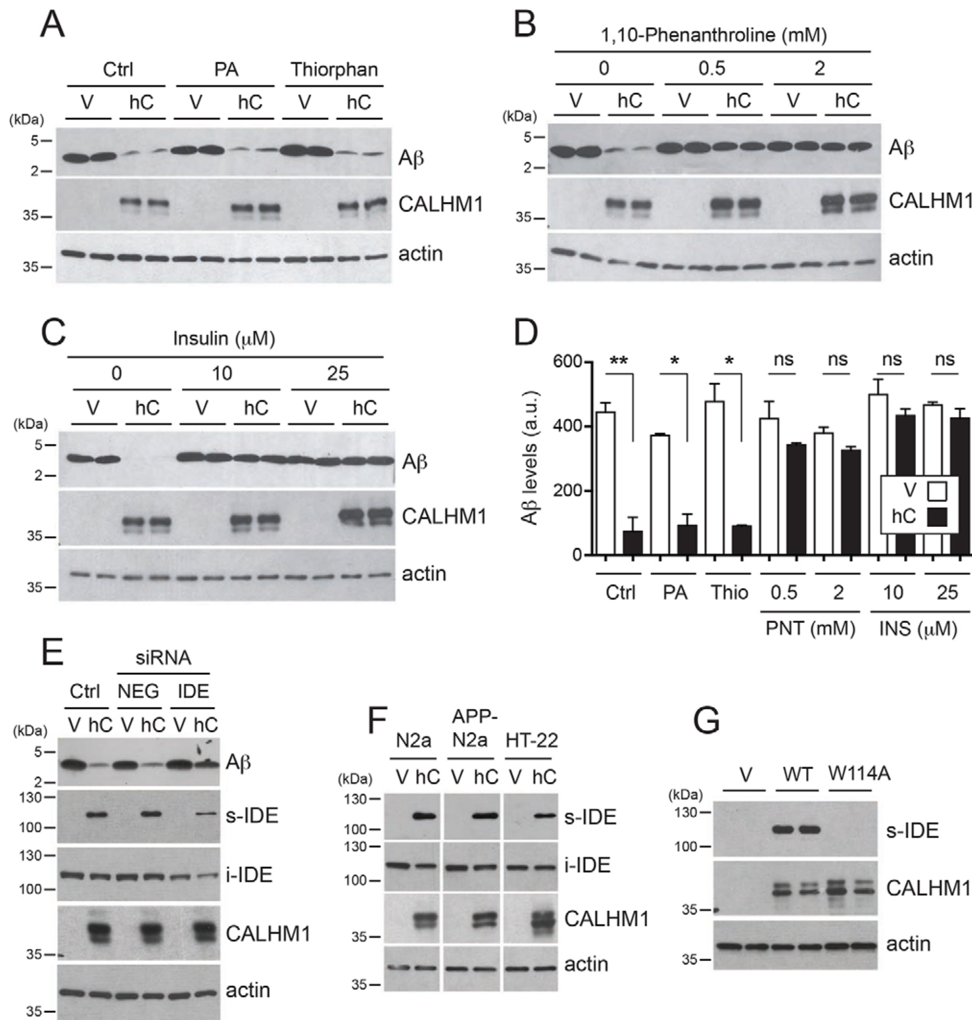

Fig. 3. CALHM1 promotes extracellular Aβ degradation by IDE. (A–C) APP-N2a cells transfected with control vector (V) or human CALHM1 (hC) were preincubated or not for 30 min with phosphoramidon [PA, 100 µM, (A)], thiorphan [10 µM, (A)], PNT (B) or insulin (C). Cells were then stimulated for 1 h with 0.2 mM $CaCl_2$ aCSF supplemented or not with the different inhibitors and were analyzed by western blotting for the indicated proteins. (D) Densitometric analyses and quantification of Aβ levels in three to six independent measurements as in A–C, expressed in arbitrary units (a.u.). Results are mean±s.d. **P*<0.01; ***P*<0.0001 (unpaired Student's *t*-test). Thio, thiorphan; INS, insulin. (E) APP-N2a cells were co-transfected with IDE-targeting siRNA (IDE siRNA) and CALHM1 (hC), or with their respective controls, negative siRNA control (NEG siRNA) and control vector (V), respectively. Cells were then stimulated for 1 h with 0.2 mM $CaCl_2$ aCSF and analyzed by western blotting for the indicated proteins. Secreted extracellular IDE (s-IDE) and intracellular IDE (i-IDE) were also analyzed by western blotting. Ctrl, control not transfected with siRNA. (F) Naïve N2a, APP-N2a, and HT-22 cells transfected with control vector (V) or human CALHM1 (hC) were stimulated for 1 h with 0.2 mM $CaCl_2$ aCSF. Cells were then analyzed by western blotting for the indicated proteins. (G) APP-N2a cells transfected with control vector (V), WT-CALHM1 or W114A-CALHM1 were stimulated for 1 h with 0.2 mM $CaCl_2$ aCSF and analyzed by western blotting for the indicated proteins. Western blotting results in A–C and E–G are representative of at least three independent experiments.

lower levels of Aβ degradation activity in CALHM1-deficient mice, compared to WT mice (Fig. 4A,B). Aβ degradation activity measured in this *in vitro* assay in the membrane-associated brain homogenates was almost entirely sensitive to insulin and PNT (Fig. 4C), indicating that the proteolytic activity directed against Aβ measured in this assay is mostly due to IDE. Insulin degradation activity in these homogenates was significantly inhibited by PNT, confirming that IDE is also the main proteolytic activity directed against insulin in our assay (Fig. 4D). In line with the results obtained for synthetic Aβ degradation, *Calhm1*-KO brain homogenates showed a clear trend of reduction in insulin degradation activity, compared to WT brain homogenates (Fig. 4E).

The APP intracellular domain (AICD) is the C-terminal fragment of APP produced by γ-secretase (Marambaud and Robakis, 2005). Previous studies have found that IDE targets AICD for degradation in cell cultures (Edbauer et al., 2002) and *in vivo* in mice (Farris et al., 2003; Miller et al., 2003). IDE subcellular localization is unconventional and the exact trafficking pathways leading to its presence both outside the cell and in the cytosol remain to be clearly defined. Using subcellular fractionation, we confirmed that intracellular IDE was mainly found as a soluble pool in the cytosol (Fig. 5A). This localization of IDE in the cytosol is consistent with its role in AICD degradation (Edbauer et al., 2002; Vekrellis et al., 2000).

AICD metabolism (production and degradation), like the metabolism of other protein fragments produced by γ-secretase, can be followed *in vitro* by incubating membranes isolated from cell or brain tissue homogenates at 37°C (Marambaud et al., 2003). Using this membrane assay, we preincubated brain homogenates *in vitro* for 2 h to produce the γ-secretase inhibitor-sensitive AICD

Journal of Cell Science

 Journal of Cell Science (2015) 128, 2330-2338 doi:10.1242/jcs.167270

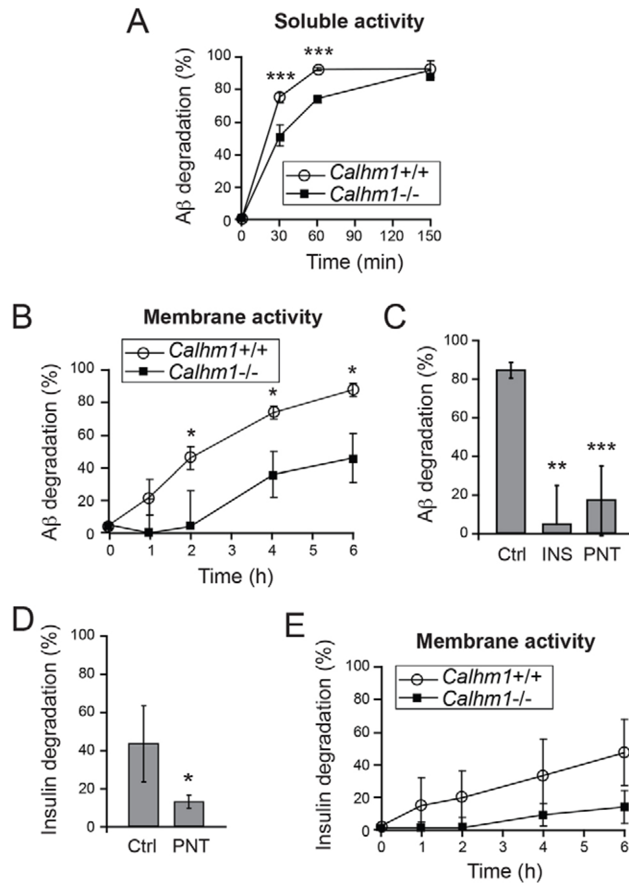

Fig. 4. IDE activity in CALHM1-deficient mouse brains. (A–E) *In vitro* degradation assay of synthetic Aβ42 (A–C) and recombinant insulin (D,E) in soluble (A) or membrane-associated (B–E) brain homogenates from 6-month-old $Calhm1^{+/+}$ and $Calhm1^{-/-}$ littermate mice. Aβ42 and insulin levels were measured by ELISA and expressed as a degradation percentage compared with the 0 h time point. Aβ42 (C) and insulin (D) degradation in membrane-associated fractions of $Calhm1^{+/+}$ mouse brains were determined in the presence or absence of insulin [INS, 10 μM, (C)] or PNT (5 mM, C,D) at the 6 h time point. Results are mean±s.d. [*n*=3 or 4 (A,B,E); *n*=4 or 5 (C,D)]. $^*P<0.05$, $^{**}P<0.01$, $^{***}P<0.001$ (ANOVA Bonferroni post-hoc tests, A,B,E, or Student's *t*-tests, C,D).

fragment (Fig. 5B). AICD degradation was then assessed by incubating the homogenates for 5 h (Fig. 5B, 0, 2, 5 h). In these conditions, a decrease of AICD levels was readily detectable and the rate of AICD degradation could be quantified (Fig. 5B,C). Importantly, the decrease over time of AICD levels was fully protected by PNT treatment (Fig. 5B), confirming that IDE is the enzyme responsible for AICD degradation in this assay. Because no increase in AICD levels were observed over time in the presence of PNT, we concluded that AICD production after the 2 h preincubation reached saturation levels (Fig. 5B). Under these conditions, we found a significant decrease in AICD degradation activity in *Calhm1*-KO brain membranes, compared to membranes isolated from WT brains (Fig. 5B,C). Taken together, these data show that CALHM1 deficiency decreases brain IDE activity.

CALHM1 deficiency increases endogenous Aβ and AICD levels in the mouse brain

Aβ in the brain is mainly produced by neurons. IDE, however, is ubiquitously expressed and could potentially control extracellular Aβ levels by being released from cell types other than neurons. Because

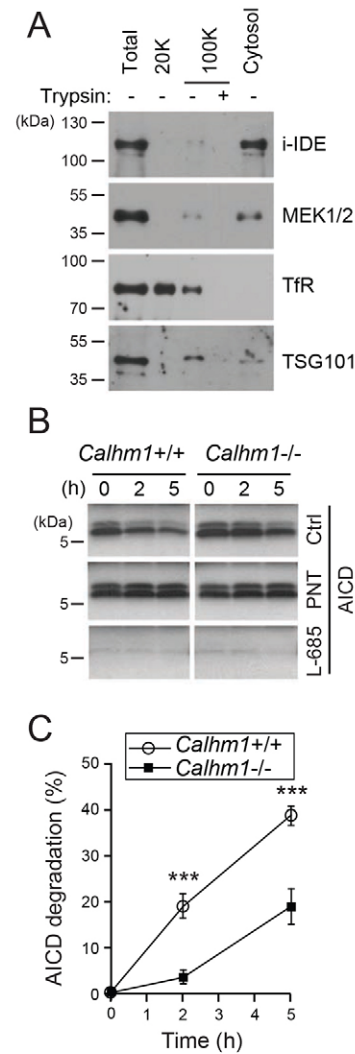

Fig. 5. AICD degradation in CALHM1-deficient mouse brains. (A) IDE subcellular localization analysis by differential centrifugation in N2a cells. Cell homogenates (Total) were centrifuged at 20,000 ***g*** to isolate vesicles of plasma membrane origin and lysosomes [20 K, enriched in the cell surface marker transferrin receptor (TfR)]. Supernatant was then centrifuged at 100,000 ***g*** to isolate the endosomes and multivesicular bodies (100 K, enriched in both transferrin receptor and the ESCRT-I subunit TSG101). The final supernatant contained the soluble cytosolic proteins (cytosol, enriched in the cytosolic markers MEK1 and MEK2). Intact vesicles from the 100 K fraction were trypsinized to degrade proteins exposed to the cytosol (Trypsin). Equal amounts of proteins from the different fractions were then analyzed by western blotting using antibodies directed against the indicated proteins. i-IDE, intracellular IDE. Note that i-IDE was not significantly associated with intracellular vesicles retrieved at 20,000 ***g*** (i.e. the lysosomes and vesicles of plasma membrane origin) or at 100,000 ***g*** (i.e. the endosomes and multivesicular bodies), but instead was mainly found as a soluble pool in the cytosol. (B,C) An *in vitro* AICD degradation assay in brain homogenates of 6-month-old $Calhm1^{+/+}$ and $Calhm1^{-/-}$ littermate mice. Representative western blotting of AICD levels over time during the assay in the absence or presence of PNT (5 mM) or L-685,458 (γ-secretase inhibitor, 5 μM) is shown in B. Western blotting quantification of three independent experiments as in B, expressed as a percentage of AICD degradation compared with the 0 time point, is shown in C. Results are mean±s.d. (*n*=3; $^{***}P<0.001$; ANOVA Bonferroni post-hoc tests). Western blotting results in A and B are representative of three independent experiments.

CALHM1 is expressed in cerebral neurons (Dreses-Werringloer et al., 2013; Ma et al., 2012), we asked whether CALHM1 deficiency affects the steady-state levels of endogenously produced Aβ in isolated whole

Journal of Cell Science

 Journal of Cell Science (2015) 128, 2330-2338 doi:10.1242/jcs.167270

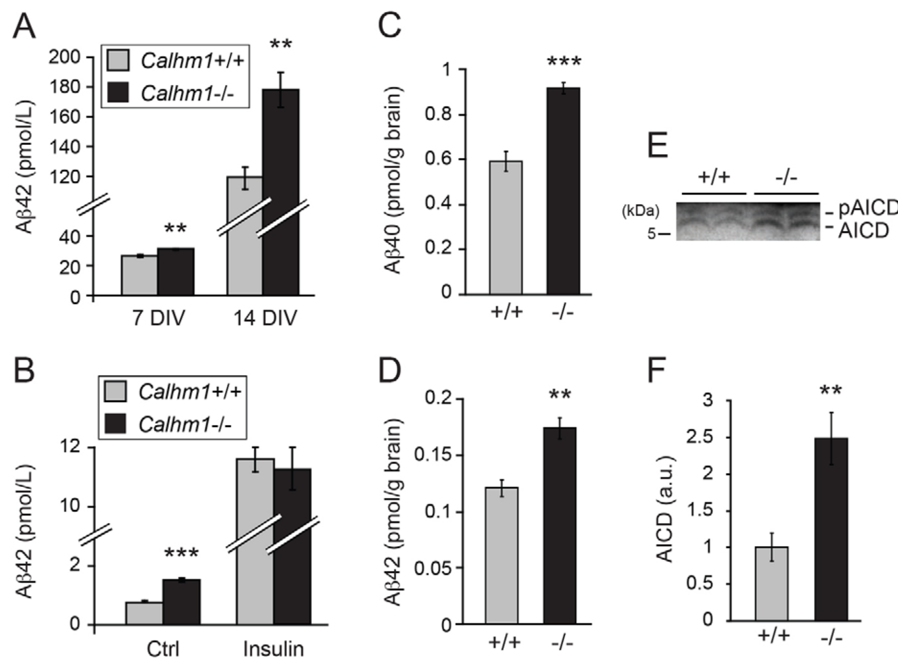

Fig. 6. Endogenous Aβ and AICD levels in CALHM1-deficient mouse brains. (A) Steady-state levels of extracellular Aβ42 secreted by primary neurons obtained from *Calhm1*$^{+/+}$ and *Calhm1*$^{-/-}$ mouse brains and maintained in culture for 7 and 14 days *in vitro* (DIV; results are mean±s.d.; *n*=4; ***P*<0.005; Student's *t*-test). (B) Extracellular Aβ42 levels after a 24 h secretion in the presence or absence of insulin (10 µM) in 14 DIV primary neurons obtained from *Calhm1*$^{+/+}$ and *Calhm1*$^{-/-}$ mouse brains (results are mean±s.d.; *n*=6; ****P*<0.0005; Student's *t*-test). (C–E) Endogenous Aβ40 (C) and Aβ42 (D) ELISA (results are mean±s.e.m.; *n*=8 or 9; ****P*<0.001; ***P*<0.01; Student's *t*-test), and AICD western blotting (E) in brains of 15-month-old *Calhm1*$^{+/+}$ and *Calhm1*$^{-/-}$ littermates. pAICD, phosphorylated form of AICD (Farris et al., 2003). Western blotting results in E are representative of three independent experiments. (F) Western blotting quantification of AICD levels as in E expressed in arbitrary units (a.u.; results are mean±s.d.; *n*=3; ***P*<0.002; Student's *t*-test).

forebrain primary neuron cultures. We found that *Calhm1*-KO neurons accumulated significantly more Aβ42 over time than neurons isolated from WT mice (Fig. 6A). The effect of CALHM1 deficiency on Aβ42 accumulation was abolished by the IDE competitive inhibitor insulin (Fig. 6B), indicating that the increase in Aβ42 in *Calhm1*-KO neurons was due to a deficit in IDE-mediated degradation. These data not only confirm that endogenous CALHM1 promotes Aβ degradation by IDE, but also reveal that this mechanism is controlled by neurons. To go further, we measured and quantified the steady-state levels of endogenous Aβ40 and Aβ42 in *Calhm1*-KO brains. CALHM1 deficiency resulted in a significant increase of Aβ40 and Aβ42 levels [51% increase of Aβ40 – WT, 0.6±0.04 pmol/g versus KO, 0.9±0.02 pmol/g, *P*=0.0005; 40% increase of Aβ42 – WT, 0.12±0.007 pmol/g versus KO, 0.17±0.009 pmol/g, *P*=0.0067 (mean±s.e.m., Student's *t*-test); Fig. 6C,D]. Furthermore, the total levels of AICD were increased in *Calhm1*-KO brain homogenates, compared to homogenates isolated from WT brains (Fig. 6E,F). Thus, CALHM1 deficiency increases endogenous Aβ and AICD levels in the mouse brain.

DISCUSSION

In the current study, we show that CALHM1 is a repressor of Aβ accumulation in cell lines and *in vivo* in the mouse brain. We determined that CALHM1 acted by promoting an extracellular mechanism of Aβ degradation. Using pharmacological and RNAi approaches, we identified IDE as the protease solely responsible for CALHM1-dependent Aβ degradation. These results were corroborated by an analysis of *Calhm1*-KO mice, which displayed a consistent decrease in cerebral IDE activity accompanied by a significant elevation of endogenous Aβ levels in both the whole brain and primary neurons. Additional investigation in cell cultures revealed that CALHM1 promoted IDE-mediated Aβ degradation by triggering IDE secretion.

The importance of these results is twofold. A main therapeutic strategy for drug development in Alzheimer's disease is focusing on approaches aimed at interfering with Aβ accumulation in the brain (Citron, 2010). Furthermore, ion channels, and, more specifically, cell surface ion channels that are more easily accessible, are targets of choice for drug development (Clare, 2010). In this context, our data not only reveal new insights into CALHM1 biology and its relevance to Alzheimer's disease pathogenesis, but also warrant further investigation aimed at determining whether anti-amyloidogenic CALHM1 activating interventions can be identified.

The localization and substrate accessibility of IDE is complex and its exact trafficking is only partially understood (Leissring and Turner, 2013). IDE can be found in the cytosol, where it degrades AICD, or outside the cell, where it regulates the catabolism of several soluble peptides (Turner and Nalivaeva, 2007). At the mechanistic level, our study identified a role for CALHM1 in IDE cellular secretion. By using a cell membrane fractionation method, we found a reduction in the activity of not only soluble IDE but also membrane-associated IDE in the *Calhm1*-KO brain. Our data therefore suggest that CALHM1 could also be involved in other mechanisms of IDE activation or substrate accessibility, not only extracellularly but also in the cytosol, as suggested by the observed effect of CALHM1 on AICD levels. Further studies will be needed to address this possibility and determine which mechanisms of IDE maturation or trafficking might also be modulated by CALHM1.

We further determined that CALHM1 ion channel and extracellular Ca^{2+} are required for the CALHM1 anti-amyloidogenic effect. Indeed, pharmacological and genetic approaches (using Ruthenium Red, Zn^{2+} or inactive CALHM1 mutants) revealed that CALHM1 promoted IDE-mediated Aβ clearance through its ion channel properties. Moreover, manipulation of $[Ca^{2+}]_o$ revealed that extracellular Ca^{2+} was required for the CALHM1 anti-amyloidogenic effect. These data strongly support the notion that Ca^{2+} influx through CALHM1 is the trigger for the observed effect on Aβ clearance by IDE. It is important to note, however, that CALHM1 has been reported to form a large pore that can allow significant permeabilities for other ions, such as Na^+, K^+ and Cl^-, or for larger molecules, such as ATP (Ma et al., 2012; Siebert et al., 2013; Taruno et al., 2013). CALHM1 permeability activation is therefore expected to result in the control of multiple signaling pathways that could potentially also contribute to different mechanisms of IDE activation and to the observed effect on Aβ clearance. In this context, additional studies will have to determine whether Ca^{2+} influx through CALHM1 is the only trigger for Aβ clearance or whether other

Journal of Cell Science

Journal of Cell Science (2015) 128, 2330-2338 doi:10.1242/jcs.167270

pathways controlled by CALHM1 permeability for different ions or molecules are also required.

In summary, this work shows for the first time that CALHM1 is an ion channel that has anti-amyloidogenic properties *in vivo* in the mammalian brain. Specifically, we found that CALHM1 promoted a neuronal and Ca^{2+}-dependent mechanism of extracellular Aβ degradation by IDE. These data warrant further investigation aimed at determining whether CALHM1 ion channel activity can be pharmacologically targeted for promoting amyloid clearance in the Alzheimer's disease brain.

MATERIALS AND METHODS

Chemicals, plasmids, and antibodies

Ruthenium Red, $ZnCl_2$, NH_4Cl, chloroquine, 1,10-phenanthroline and insulin were purchased from Sigma-Aldrich. Phosphoramidon was from Cayman Chemical and thiorphan from Enzo Life Sciences. BFA was from Epicentre Technologies. Plasmids containing Myc- or V5-tagged WT and mutant (N140A and W114A) human and mouse CALHM1 cDNAs were as described previously (Dreses-Werringloer et al., 2008, 2013). V5-tagged D121R-CALHM1 mutant was created by using the QuikChange II site-directed mutagenesis kit (Agilent Technologies) and confirmed by sequencing. Anti-Aβ1-17 (6E10) and anti-Aβ17-24 (4G8) antibodies were from Covance, and anti-APP1–200 antibody (LN27) was from Zymed Laboratories Inc. Anti-APP C-terminal domain antibody (R1) was as described previously (Vingtdeux et al., 2010). Anti-IDE and anti-TSG101 antibodies were from Abcam, anti-Myc and the antibody against both MEK1 and MEK2 (also known as MAP2K1 and MAP2K2, respectively) was from Cell Signaling Technology, anti-V5 antibody was from Invitrogen, anti-actin antibody was from BD Transduction Laboratories, and anti-transferrin receptor antibody was from Invitrogen.

Mice

All animal experiments were performed according to procedures approved by the Feinstein Institute for Medical Research Institutional Animal Care and Use Committee. The *Calhm1*-KO mice were as described previously (Dreses-Werringloer et al., 2013; Taruno et al., 2013).

Cell cultures, transfections, and drug treatments

Naïve N2a cells were obtained from the ATCC. N2a cells stably transfected with human APP695 (APP-N2a) and HT-22 cells were described and maintained as reported previously (Dreses-Werringloer et al., 2008). Cells were transiently transfected in complete medium without antibiotics with the different CALHM1 cDNAs using Lipofectamine 2000 reagent (Invitrogen), as per the manufacturer's instructions. At 16 h post-transfection, cells were incubated for 1 h in aCSF buffer (in mM: 120 NaCl, 26 $NaHCO_3$, 1 NaH_2PO_4, 2.5 KCl, 1.3 $MgSO_4$, 10 D-Glucose, and 0.2 $CaCl_2$) to activate CALHM1. IDE RNAi was performed by transfection of IDE-targeting siRNA (Silencer Select, Ambion, Life Technologies) or negative control siRNA (Silencer Select, Ambion) for 24 h with Lipofectamine RNAiMAX reagent (Invitrogen). Primary neurons from day 17 embryos were prepared as previously described (Dreses-Werringloer et al., 2013; Vingtdeux et al., 2010).

Intracellular Ca^{2+} measurements

$[Ca^{2+}]_i$ was measured using Fluo-4 (Fluo-4 NW Ca^{2+} Assay Kit, Life Technologies) as described previously (Dreses-Werringloer et al., 2013). Transiently transfected HT-22 cells were incubated for the indicated times in aCSF buffer containing 0.2 mM $CaCl_2$ and supplemented or not with 2 mM EGTA. In one experimental setting, Ca^{2+} concentration was restored in EGTA-supplemented aCSF buffer by adding 5 mM $CaCl_2$.

Western blot and immunoprecipitation analyses

Cells were washed with phosphate-buffered saline (PBS) and solubilized in RIPA buffer (Millipore) supplemented with 1× Complete protease inhibitor mixture (Roche Applied Science). Depending on the primary antibody used, 5–20 µg of cell extracts were analyzed by SDS-PAGE. Conditioned medium containing secreted total Aβ, secreted (s)APPα and IDE was analyzed by direct western blots, as described previously (Vingtdeux et al., 2010). Intracellular Aβ levels were analyzed in cells harvested by trypsinization and by immunoprecipitation using the 4G8 antibody, as described previously (Vingtdeux et al., 2010).

Brain IDE *in vitro* degradation assays

Brains from 6-month-old *Calhm1*$^{+/+}$ and *Calhm1*$^{-/-}$ mice were homogenized in 8 volumes (w/v) of 250 mM sucrose in 50 mM Tris-HCl pH 7.4. Nuclei were pelleted and the supernatants were centrifuged at 100,000 ***g*** for 1 h. Resulting supernatants were saved as soluble fractions and membrane pellets were resuspended in 100 mM Na_2CO_3, pH 11.3 and centrifuged at 100,000 ***g*** for 1 h. Pellets were resuspended in 50 mM Tris-HCl pH 7.4 and sonicated. Protein concentration in soluble and membrane fractions were evaluated using BCA assay. To quantify proteolysis of Aβ by brain fractions, 100 pM of synthetic human Aβ1-42 (Invitrogen) was incubated at 37°C with 100 µg/ml proteins of soluble or membrane fractions. At each time point, an aliquot of the sample was removed and stored at −80°C until analysis. To measure proteolysis of insulin, 100 pM of recombinant human insulin (Sigma) was incubated at 37°C with 50 µg/ml of proteins from the membrane fraction. ELISA was used to determine Aβ (Wako) and insulin (ALPCO Diagnostics) concentrations.

Subcellular fractionation

N2a cells were homogenized in Buffer A (10 mM NaCl, 1.5 mM $MgCl_2$, 2 mM DTT, 10 mM Tris-HCl pH 7.4) using 50 strokes of the pestle of a tight-fitting Dounce. Buffer B (525 mM mannitol, 175 mM sucrose, 2.5 mM EDTA, 12.5 mM Tris-HCl, pH 7.4) was then added at a 4:10 ratio to the cell homogenate in Buffer A. The resulting homogenate was centrifuged at 1300 ***g*** for 10 min to remove the nuclei. Supernatant was centrifuged at 20,000 ***g*** for 45 min to isolate a first fraction (denoted 20 K, enriched in the cell surface marker transferrin receptor). Supernatant was then centrifuged at 100,000 ***g*** for 3 h to isolate a second fraction (denoted 100 K, enriched in both transferrin receptor and the ESCRT-I subunit TSG101). The final supernatant contained the soluble cytosolic proteins and was enriched in the cytosolic markers MEK1 and MEK2. Intact vesicles from the 100 K fraction were trypsinized (0.25% trypsin for 10 min at 37°C) to degrade proteins exposed to the cytosol.

In vitro AICD degradation assay

Cell membranes were obtained from brains of 6-month-old *Calhm1*$^{+/+}$ and *Calhm1*$^{-/-}$ mice using the *in vitro* γ-secretase assay described previously (Marambaud et al., 2003). AICD was generated by incubation of the membrane preparations at 37°C for 2 h in a volume of 25 µl/assay. Samples were further incubated for 5 h to monitor AICD degradation. AICD levels were then analyzed by western blotting using the R1 antibody.

Endogenous Aβ40 and Aβ42 quantification

Endogenous Aβ1-40 and Aβ1-42 levels were assessed in total brain homogenates of 15-month-old *Calhm1*$^{+/+}$ and *Calhm1*$^{-/-}$ littermate mice. Aβ1-40 and Aβ1-42 concentrations were determined by ELISA (Wako).

Acknowledgements

We thank Dr Luca Giliberto (The Feinstein Institute for Medical Research, Manhasset, New York 11030, USA) for critical reading of the manuscript.

Competing interests

The authors declare no competing or financial interests.

Author contributions

V.V., L.B. and P.M. designed research. V.V., P.C., H.Z., S.R. and P.M. performed research. V.V. and P.M. analyzed data and wrote the paper.

Funding

This work was supported by a KeySpan award; a Feinstein Institute for Medical Research Competitive Faculty award and the National Institutes of Health [grant number R01AG042508 to P.M.]. Deposited in PMC for release after 12 months.

References

Aguilar, D., Skrabanek, L., Gross, S. S., Oliva, B. and Campagne, F. (2008). Beyond tissueInfo: functional prediction using tissue expression profile similarity searches. *Nucleic Acids Res.* **36**, 3728-3737.

Benilova, I., Gallardo, R., Ungureanu, A.-A., Castillo Cano, V., Snellinx, A., Ramakers, M., Bartic, C., Rousseau, F., Schymkowitz, J. and De Strooper, B. (2014). The Alzheimer disease protective mutation A2T modulates kinetic and thermodynamic properties of amyloid-β (Aβ) aggregation. *J. Biol. Chem.* **289**, 30977-30989.

Berridge, M. J. (2010). Calcium hypothesis of Alzheimer's disease. *Pflugers Arch. Eur. J. Physiol.* **459**, 441-449.

Chapuis, J., Vingtdeux, V., Campagne, F., Davies, P. and Marambaud, P. (2011). Growth arrest-specific 1 binds to and controls the maturation and processing of the amyloid-beta precursor protein. *Hum. Mol. Genet.* **20**, 2026-2036.

Citron, M. (2010). Alzheimer's disease: strategies for disease modification. *Nat. Rev. Drug Discov.* **9**, 387-398.

Clare, J. J. (2010). Targeting ion channels for drug discovery. *Discov. Med.* **9**, 253-260.

de Leon, M. J., Mosconi, L., Blennow, K., Desanti, S., Zinkowski, R., Mehta, P. D., Pratico, D., Tsui, W., Saint Louis, L. A., Sobanska, L. et al. (2007). Imaging and CSF studies in the preclinical diagnosis of Alzheimer's disease. *Ann. N. Y. Acad. Sci.* **1097**, 114-145.

De Strooper, B., Vassar, R. and Golde, T. (2010). The secretases: enzymes with therapeutic potential in Alzheimer disease. *Nat. Rev. Neurol.* **6**, 99-107.

Dreses-Werringloer, U., Lambert, J.-C., Vingtdeux, V., Zhao, H., Vais, H., Siebert, A., Jain, A., Koppel, J., Rovelet-Lecrux, A., Hannequin, D. et al. (2008). A polymorphism in CALHM1 influences Ca2+ homeostasis, Abeta levels, and Alzheimer's disease risk. *Cell* **133**, 1149-1161.

Dreses-Werringloer, U., Vingtdeux, V., Zhao, H., Chandakkar, P., Davies, P. and Marambaud, P. (2013). CALHM1 controls the Ca^{2+}-dependent MEK, ERK, RSK and MSK signaling cascade in neurons. *J. Cell Sci.* **126**, 1199-1206.

Duyckaerts, C., Delatour, B. and Potier, M.-C. (2009). Classification and basic pathology of Alzheimer disease. *Acta Neuropathol.* **118**, 5-36.

Edbauer, D., Willem, M., Lammich, S., Steiner, H. and Haass, C. (2002). Insulin-degrading enzyme rapidly removes the beta-amyloid precursor protein intracellular domain (AICD). *J. Biol. Chem.* **277**, 13389-13393.

Espuny-Camacho, I., Dominguez, D., Merchiers, P., Van Rompaey, L., Selkoe, D. and De Strooper, B. (2010). Peroxisome proliferator-activated receptor gamma enhances the activity of an insulin degrading enzyme-like metalloprotease for amyloid-beta clearance. *J. Alzheimers Dis.* **20**, 1119-1132.

Farris, W., Mansourian, S., Chang, Y., Lindsley, L., Eckman, E. A., Frosch, M. P., Eckman, C. B., Tanzi, R. E., Selkoe, D. J. and Guenette, S. (2003). Insulin-degrading enzyme regulates the levels of insulin, amyloid beta-protein, and the beta-amyloid precursor protein intracellular domain in vivo. *Proc. Natl. Acad. Sci. USA* **100**, 4162-4167.

Giedraitis, V., Glaser, A., Sarajärvi, T., Brundin, R., Gunnarsson, M. D., Schjeide, B.-M., Tanzi, R. E., Helisalmi, S., Pirttilä, T., Kilander, L. et al. (2010). CALHM1 P86L polymorphism does not alter amyloid-beta or tau in cerebrospinal fluid. *Neurosci. Lett.* **469**, 265-267.

Haass, C. and Selkoe, D. J. (2007). Soluble protein oligomers in neurodegeneration: lessons from the Alzheimer's amyloid beta-peptide. *Nat. Rev. Mol. Cell Biol.* **8**, 101-112.

Hardy, J. and Selkoe, D. J. (2002). The amyloid hypothesis of Alzheimer's disease: progress and problems on the road to therapeutics. *Science* **297**, 353-356.

Jonsson, T., Atwal, J. K., Steinberg, S., Snaedal, J., Jonsson, P. V., Bjornsson, S., Stefansson, H., Sulem, P., Gudbjartsson, D., Maloney, J. et al. (2012). A mutation in APP protects against Alzheimer's disease and age-related cognitive decline. *Nature* **488**, 96-99.

Kauwe, J. S., Cruchaga, C., Bertelsen, S., Mayo, K., Latu, W., Nowotny, P., Hinrichs, A. L., Fagan, A. M., Holtzman, D. M., Goate, A. M. et al. (2010). Validating predicted biological effects of Alzheimer's disease associated SNPs using CSF biomarker levels. *J. Alzheimers Dis.* **21**, 833-842.

Knops, J., Gandy, S., Greengard, P., Lieberburg, I. and Sinha, S. (1993). Serine phosphorylation of the secreted extracellular domain of APP. *Biochem. Biophys. Res. Commun.* **197**, 380-385.

Koppel, J., Campagne, F., Vingtdeux, V., Dreses-Werringloer, U., Ewers, M., Rujescu, D., Hampel, H., Gordon, M. L., Christen, E., Chapuis, J. et al. (2011). CALHM1 P86L polymorphism modulates CSF Aβ levels in cognitively healthy individuals at risk for Alzheimer's disease. *Mol. Med.* **17**, 974-979.

Lambert, J.-C. and Amouyel, P. (2011). Genetics of Alzheimer's disease: new evidences for an old hypothesis? *Curr. Opin. Genet. Dev.* **21**, 295-301.

Lambert, J. C., Sleegers, K., González-Pérez, A., Ingelsson, M., Beecham, G. W., Hiltunen, M., Combarros, O., Bullido, M. J., Brouwers, N., Bettens, K. et al. (2010). The CALHM1 P86L polymorphism is a genetic modifier of age at onset in Alzheimer's disease: a meta-analysis study. *J. Alzheimers Dis.* **22**, 247-255.

Langhans, M., Hawes, C., Hillmer, S., Hummel, E. and Robinson, D. G. (2007). Golgi regeneration after brefeldin A treatment in BY-2 cells entails stack enlargement and cisternal growth followed by division. *Plant Physiol.* **145**, 527-538.

Leissring, M. A. and Turner, A. J. (2013). Regulation of distinct pools of amyloid β-protein by multiple cellular proteases. *Alzheimers Res. Ther.* **5**, 37.

Lippincott-Schwartz, J., Yuan, L. C., Bonifacino, J. S. and Klausner, R. D. (1989). Rapid redistribution of Golgi proteins into the ER in cells treated with brefeldin A: evidence for membrane cycling from Golgi to ER. *Cell* **56**, 801-813.

Ma, Z., Siebert, A. P., Cheung, K.-H., Lee, R. J., Johnson, B., Cohen, A. S., Vingtdeux, V., Marambaud, P. and Foskett, J. K. (2012). Calcium homeostasis modulator 1 (CALHM1) is the pore-forming subunit of an ion channel that mediates extracellular Ca2+ regulation of neuronal excitability. *Proc. Natl. Acad. Sci. USA* **109**, E1963-E1971.

Maloney, J. A., Bainbridge, T., Gustafson, A., Zhang, S., Kyauk, R., Steiner, P., van der Brug, M., Liu, Y., Ernst, J. A., Watts, R. J. et al. (2014). Molecular mechanisms of Alzheimer disease protection by the A673T allele of amyloid precursor protein. *J. Biol. Chem.* **289**, 30990-31000.

Marambaud, P. and Robakis, N. K. (2005). Genetic and molecular aspects of Alzheimer's disease shed light on new mechanisms of transcriptional regulation. *Genes Brain Behav.* **4**, 134-146.

Marambaud, P., Wen, P. H., Dutt, A., Shioi, J., Takashima, A., Siman, R. and Robakis, N. K. (2003). A CBP binding transcriptional repressor produced by the PS1/epsilon-cleavage of N-cadherin is inhibited by PS1 FAD mutations. *Cell* **114**, 635-645.

Miller, B. C., Eckman, E. A., Sambamurti, K., Dobbs, N., Chow, K. M., Eckman, C. B., Hersh, L. B. and Thiele, D. L. (2003). Amyloid-beta peptide levels in brain are inversely correlated with insulysin activity levels in vivo. *Proc. Natl. Acad. Sci. USA* **100**, 6221-6226.

Nixon, R. A., Yang, D.-S. and Lee, J.-H. (2008). Neurodegenerative lysosomal disorders: a continuum from development to late age. *Autophagy* **4**, 590-599.

Pflanzner, T., Kuhlmann, C. R. and Pietrzik, C. U. (2010). Blood-brain-barrier models for the investigation of transporter- and receptor-mediated amyloid-β clearance in Alzheimer's disease. *Curr. Alzheimer Res.* **7**, 578-590.

Rusakov, D. A. and Fine, A. (2003). Extracellular Ca2+ depletion contributes to fast activity-dependent modulation of synaptic transmission in the brain. *Neuron* **37**, 287-297.

Serrano-Pozo, A., Frosch, M. P., Masliah, E. and Hyman, B. T. (2011). Neuropathological alterations in Alzheimer disease. *Cold Spring Harb. Perspect. Med.* **1**, a006189.

Siebert, A. P., Ma, Z., Grevet, J. D., Demuro, A., Parker, I. and Foskett, J. K. (2013). Structural and functional similarities of calcium homeostasis modulator 1 (CALHM1) ion channel with connexins, pannexins, and innexins. *J. Biol. Chem.* **288**, 6140-6153.

Tanis, J. E., Ma, Z., Krajacic, P., He, L., Foskett, J. K. and Lamitina, T. (2013). CLHM-1 is a functionally conserved and conditionally toxic Ca2+-permeable ion channel in Caenorhabditis elegans. *J. Neurosci.* **33**, 12275-12286.

Taruno, A., Vingtdeux, V., Ohmoto, M., Ma, Z., Dvoryanchikov, G., Li, A., Adrien, L., Zhao, H., Leung, S., Abernethy, M. et al. (2013). CALHM1 ion channel mediates purinergic neurotransmission of sweet, bitter and umami tastes. *Nature* **495**, 223-226.

Turner, A. J. and Nalivaeva, N. N. (2007). New insights into the roles of metalloproteinases in neurodegeneration and neuroprotection. *Int. Rev. Neurobiol.* **82**, 113-135.

Vekrellis, K., Ye, Z., Qiu, W. Q., Walsh, D., Hartley, D., Chesneau, V., Rosner, M. R. and Selkoe, D. J. (2000). Neurons regulate extracellular levels of amyloid beta-protein via proteolysis by insulin-degrading enzyme. *J. Neurosci.* **20**, 1657-1665.

Vingtdeux, V., Giliberto, L., Zhao, H., Chandakkar, P., Wu, Q., Simon, J. E., Janle, E. M., Lobo, J., Ferruzzi, M. G., Davies, P. et al. (2010). AMP-activated protein kinase signaling activation by resveratrol modulates amyloid-beta peptide metabolism. *J. Biol. Chem.* **285**, 9100-9113.

Vingtdeux, V., Tanis, J. E., Chandakkar, P., Zhao, H., Dreses-Werringloer, U., Campagne, F., Foskett, J. K. and Marambaud, P. (2014). Effect of the CALHM1 G330D and R154H Human Variants on the Control of Cytosolic Ca2+ and Aβ Levels. *PLoS ONE* **9**, e112484.

Zolezzi, J. M., Bastías-Candia, S., Santos, M. J. and Inestrosa, N. C. (2014). Alzheimer's disease: relevant molecular and physiopathological events affecting amyloid-β brain balance and the putative role of PPARs. *Front. Aging Neurosci.* **6**, 176.